Assessing and Characterizing Carbon Storage in Wetlands of the Guangdong–Hong Kong–Macau Greater Bay Area, China, During 1995–2020

Yawen Deng, Weiguo Jiang, Zhifeng Wu, *Member, IEEE*, Kaifeng Peng, Ziyan Ling, Zhuo Li, and Xiaoya Wang

***Abstract*—Wetland carbon storage plays an essential role in the global carbon cycle. However, in recent decades, intensive human activities and rapid urbanization have reduced wetland C stocks in the Guangdong–Hong Kong–Macau Greater Bay Area (GBA). Long-term assessment of carbon storage in the wetland ecosystems of the GBA is needed for promoting regional sustainable development. Therefore, we proposed a framework integrating the integrated valuation of ecosystem services and tradeoffs (InVEST) model and water inundation frequency, which was retrieved via multiple index water detection rule based on Google Earth Engine platform, to estimate yearly carbon storage in wetlands across the GBA at a 30-m spatial resolution during 1995–2020. The incorporation of water inundation frequency in estimating carbon storage in wetlands presents features of long time series and higher temporal frequency. The results showed that: first, the carbon storage of wetlands estimated by the InVEST model decreased from 33.38 to 16.64 Tg·C between 1995 and 2020 in the GBA, mainly owning to the loss of paddy fields. Second, there is a significant exponentially decreasing relationship between water inundation frequency and carbon storage density within the potential wetland extent, with the R^2 reaching 0.998, which denotes huge potential for estimating wetland carbon storage; third, annual wetland carbon storage estimated were divided into three main stages: a rapidly increasing period (1995–2004), a falling period (2005–2013), and a slightly fluctuating period (2015–2020). This research may provide references for supporting decision-making in implementing wetland-related sustainable development and carbon-neutrality policies in the GBA.**

***Index Terms*—Google Earth Engine (GEE), integrated valuation of ecosystem services and tradeoffs (InVEST) model, remote sensing (RS), wetland carbon storage, wetland change types.**

Manuscript received 19 May 2022; revised 6 July 2022; accepted 15 July 2022. Date of publication 19 July 2022; date of current version 4 August 2022. This work was supported by the National Natural Science Foundation of China under Grant U1901219, Grant U21A2022, and Grant 42071393. *(Corresponding author: Weiguo Jiang.)*

Yawen Deng, Weiguo Jiang, Kaifeng Peng, Zhuo Li, and Xiaoya Wang are with the Beijing Key Laboratory for Remote Sensing of Environment and Digital Cities, Faculty of Geographical Science, Beijing Normal University, Beijing 100875, China (e-mail: dengywbnu@qq.com; jiangweiguo@bnu.edu.cn; pengkaifeng@mail.bnu.edu.cn; lizhuo@mail.bnu.edu.cn; wangxiaoya@mail.bnu.edu.cn).

Zhifeng Wu is with the School of Geography and Remote Sensing, Guangzhou University, Guangzhou 510006, China (e-mail: zfwu@gzhu.edu.cn).

Ziyan Ling is with the School of Geography and Planning, Nanning Normal University, Nanning 530001, China, and also with the Beijing Key Laboratory for Remote Sensing of Environment and Digital Cities, Faculty of Geographical Science, Beijing Normal University, Beijing 100875, China (e-mail: lingziyan@nnnu.edu.cn).

This article has supplementary downloadable material available at https://doi.org/10.1109/JSTARS.2022.3192267, provided by the authors.

Digital Object Identifier 10.1109/JSTARS.2022.3192267

I. Introduction

WETLANDS, an important land use with abundant carbon storage, play an essential role in the global carbon cycle for its huge carbon storage capacity [1], [2]. They are vital to mitigating climate change and reducing CO_2 density due to their high potential for capturing and stoking carbon [3]–[5]. According to the Ramsar Scientific and Technical Review Panel, wetlands cover approximately 6%–9% of the planet's land surface but are estimated to store 35% of global terrestrial carbon. However, due to intensive human activities and climate changes, wetland ecosystems worldwide have been damaged much over the past few decades [6]–[8]. Their deteriorations and losses often lead to releases of greenhouse gases to the atmosphere, thus causing carbon storage loss [3]. Accurate and long time series information on the spatiotemporal dynamics of wetland carbon storage is of great significance for enhancing our understanding about ecosystem services and quantifications of environmental health assessment [3], [9], [10].

Traditional methods, such as the volume method and the box method, using in situ observations, present an opportunity to obtain the state of wetland carbon storage with high precision; however, they are costly in finance, time, and human resources, and are confined to site-scale research [11]–[13]. The rapid advancement of remote sensing technology provides a favorable and convenient tool for carbon storage estimation, thereby leading to the appearance of carbon storage estimation methods based on model simulation. The main methods of assessing carbon storage related to landscape changes include remote sensing-based model combined with the integrated valuation of ecosystem services and tradeoffs (InVEST) carbon storage and sequestration model, which has the characteristics of simple input data requirements and spatially explicit results [14]–[18]. A few studies have assessed carbon storage changes in some regions of China [14], [15], [17]. Among them, Jiang et al. [15] estimated carbon storage variations during 1995–2023 by linking the CLUE-S and the InVEST models and Liu et al. [14] assessed the terrestrial carbon storage changes with the InVEST model. However, much of them mainly put emphasis on the estimation of terrestrial carbon storage utilizing simple classification of land use types, which lacks more detailed information about wetland types.

Given that high resolution, long time series, frequent (yearly), and accurate spatial distribution information about wetlands is

relatively insufficient among plenty of open-access public land use and land cover datasets [8], [20], [21], adding the scarcity of carbon storage density parameters for different components of wetlands and wetlands in differing regions, we attempted to estimate long time series carbon storage of wetlands in the Greater Bay Area (GBA) indirectly by establishing the relationship between the water inundation frequency (WIF) and carbon storage of wetland ecosystems. In regard to carbon stock time series construction, Guo et al. [19] have attempted to predict soil organic carbon stock by hyperspectral and time-series multispectral remote sensing using a collaborative verification method, which were based on partial least square regression and extreme learning machine. This study shows the potential of highly correlated characteristics of the research object in predicting carbon stocks. However, studies on wetland carbon storage time series construction is relatively scarce. Additionally, in recent years, the advert of Google Earth Engine (GEE) cloud computing platform for processing large-scale geospatial and remote sensing big data [22], [23] has facilitated the water-related ecosystems' mapping and assessment [24]–[28]. Considering the underlying relationship between WIF and vegetation, soil organic materials, and hydrology in wetlands [29]–[31], it could be deducted that the occurrence of surface water is related to the levels of carbon storage in wetlands to a certain degree. To date, there is a lack of research on the spatiotemporal patterns of wetland ecosystem carbon storage in the GBA, and the incorporation of WIF in estimating the carbon stock in wetlands in previous studies rarely existed.

Holding abundant river networks of Pearl River Basin and diverse natural conditions, the wetland resources in the GBA are rich and diverse. As one of the four major bay areas in the world and three current megacity clusters in China, the GBA has been urbanizing rapidly over the past decades, since the implementation of China's reform and opening up in 1978 [32]–[34]. The overdevelopment and rapid urbanization of the GBA has led to significant changes in land use patterns and the disappearance of a large number of wetlands [14], thereby affecting the carbon storage of terrestrial ecosystems and other ecosystem services in this area. Therefore, it is necessary to study the spatiotemporal variations in wetland carbon storage in the GBA in recent decades to support this urban agglomeration's sustainable development.

In this study, utilizing land use maps in 1995, 2000, 2005, 2010, 2015, and 2020 as well as remotely sensing-based annual WIF datasets in the GBA during 1995–2020, the purposes of this study are as follows:

1) to assess wetland ecosystem carbon storage based on the InVEST model in the GBA in 1995, 2000, 2005, 2010, 2015, and 2020 and quantitatively analyze the spatiotemporal changes in wetland carbon stocks;
2) to propose a framework to estimate annual wetland ecosystems' carbon storage in the GBA by integrating yearly WIF information during 1995–2020;
3) to analyze the spatiotemporal variation of wetland carbon storage in the GBA among areas with varied wetland change types.

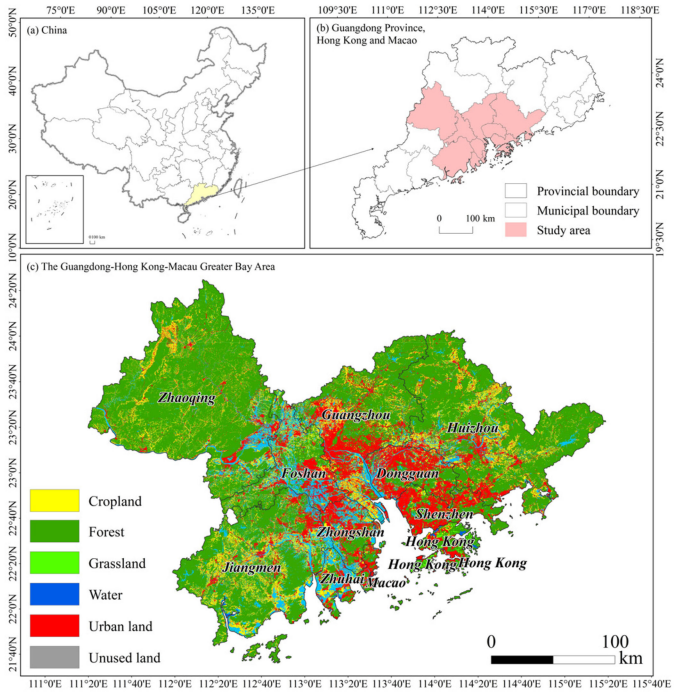

Fig. 1. Location of the Guangdong–Hong Kong–Macau GBA, China. (a) Location of Guangdong Province in China. (b) Location of the GBA. (c) Land use of the GBA in 2020.

Generally, the results of this study will improve the understanding of wetland carbon storage dynamics and provide scientific data in support of the decision-making regarding wetland conservation, restoration, management as well as socioeconomic policies toward urban sustainable development in the GBA. This work also aims to provide a concise and reliable technical process for high-resolution and long time series estimations of wetland carbon storage.

II. Materials and Methods

A. Study Area

The GBA, with a total area of approximately 56 000 km^2, is a megalopolis located in South China (latitude: 111°20′ E–115°24′ E, longitude: 21°32′ N–24°26′ N), consisting of nine cities of Guangdong province: Zhaoqing, Guangzhou, Huizhou, Foshan, Dongguan, Jiangmen, Zhongshan, Shenzhen and two special administrative regions, Hong Kong, and Macao (see Fig. 1). The climate of the GBA belongs to humid subtropical monsoon climate, with an annual precipitation of approximately 1300–2500 mm and annual average temperature of around 22 °C [33], [36], typified by abundant rainfall in hot and rainy days [35].

Surrounding the Pearl River Delta, with of approximately 86.17 million people, the GBA is the largest and the richest economic region in South China. Additionally, the GBA has a regional GDP of approximately USD 1668.8 billion at the end of 2020, which was equivalent to 12% of the GDP for all of mainland China [38]. The Chinese central government

released 'Outline Development Plan for the Guangdong–Hong Kong–Macau GBA' in February 2019 to plan the development of the GBA. The GBA is also the starting point of the Maritime Silk Road and the gateway of China to the world [37].

B. Available Land Use Maps From 1995 to 2020

In this study, we selected the years from 1995 to 2020 as the study period. To better reveal the characteristics of the wetland changes, we collected land use cover maps in 1995, 2000, 2005, 2010, 2015, and 2020 for subsequent analysis. These data were acquired from the China National Environmental Monitoring Centre (http://www.cnemc.cn/) with a spatial resolution of 30 m. According to the National Wetland Resource Survey and Technical Regulations and previous research classification, the wetlands in the GBA were classified into six types, namely, river, lake, marsh, floodplain, reservoir and pond, and paddy field. Among them, rivers, lakes, marshes, and floodplains are natural wetlands, and paddy fields and reservoirs are artificial wetlands. The temporal changes in these wetlands are shown supplementary material. We derived the spatial distribution of wetlands in the GBA for six years (see supplementary material) based on the land use datasets mentioned above as the foundation of subsequent analysis. It is clear that the area of paddy rice fields experienced a dramatic decrease of 4949.55 km^2, while the area of urban land witnessed a huge boost during 1995–2020.

C. Annual Surface Water Datasets During 1995–2020

The yearly continuous annual surface water time series from 1995 to 2020 in the GBA used in this study were already derived by employing a simple and fast water extraction method, the multiple index water detection rule [38], developed by Deng et al. [26]. This water extraction method utilizes four indices—normalized difference vegetation index (NDVI), enhanced vegetation index (EVI), modified normalized difference water index (MNDWI), and Automated Water Extraction Index (AWEI) [38]–[41] to construct the following rule: ($AWEI_{nsh}$–$AWEI_{sh}$ > -0.1) and (MNDWI $>$ NDVI or MNDWI $>$EVI) to retrieve surface water datasets in each year during the study period. The time series surface waterbody datasets used in this study are derived from existed datasets generated in another study [38], where detailed water extraction process and information about remote sensing datasets utilized could be found. Moreover, the accuracy of the surface water datasets in the GBA is relatively high, with an overall accuracy of 93.42% [38]. The spatial resolution of this surface water datasets is 30 m.

D. Methodology and Flowchart

1) Flowchart: In this study, we proposed a comprehensive research framework to estimate and analyze the long-term carbon storage changes in wetlands in the GBA, which is demonstrated in Fig. 2. The research framework can be divided into the following three main parts:

1) data preparation: three types of datasets are collected and preprocessed, such as implementing reprojection and resampling to unify the land use maps and WIF datasets;
2) we estimate wetland carbon storage via the InVEST model and conduct overlay analysis with WIF over six years to calculate the carbon density values for each WIF level, thereby constructing annual wetland carbon storage during 1995–2020 based on yearly WIF datasets;
3) we analyzed long-term carbon storage changes in areas with varied wetland change types and WIF intervals.

TABLE I
FOUR MEASUREMENTS OF CARBON DENSITY FOR EACH ECOSYSTEM TYPE USED IN THE INVEST MODEL

	Land use types	Carbon Density(Mg/hm^2)				References
		D_a	D_b	D_c	D_d	
Wetlands	Paddy field	13.50	2.70	17.34	0.00	[46]
	Water	0.21	0.00	0.00	0.00	[46]
	Marsh	17.00	8.00	14.00	1.00	[47]
	Floodplain	6.00	2.00	16.00	1.00	[47]
Non-wetlands	Forest	58.30	14.58	19.73	0.00	[46]
	Grassland	3.01	13.53	16.00	0.00	[46]
	Urban land	1.20	0.93	12.48	0.00	[46]
	Unused land	2.10	0.00	11.36	0.00	[46]

2) Carbon Storage Assessment for Wetland Ecosystems by the Invest Model: In this study, we employed the InVEST model to estimate the carbon storage in wetlands. The InVEST model assumes that each land use ecosystem corresponds to a total carbon density aggregated by aboveground, belowground, soil organic, and dead organic matter carbon densities [48]. Therefore, we could quantify the regional carbon storage based on the land use maps and carbon densities corresponding to each ecosystem. For a given pixel (*i, j*) in the land use maps, with a land use ecosystem type *M*, the carbon storage (*i, j, M*) can be calculated as follows:

$$C_{(i,j,M)} = A \times (D_a + D_b + D_c + D_d) \tag{1}$$

where *A* represents the area of the cell. D_a, D_b, D_c, and D_d are the aboveground, belowground, soil organic, and dead organic matter carbon densities for the given cell (*i, j*), respectively.

Four parameters of carbon density for differing land use types are required to feed into the InVEST carbon storage and sequestration model to estimate carbon storage, which consist of carbon density in aboveground biomass, belowground biomass, dead organic matter, and soil organic matter [48], [14]. Given that the study area in this study of Zhu et al. [46] is also within the GBA, the carbon density data in the study of Zhu et al. [46] and Ma et al. [47] were adopted in this study (see Table I), which is derived from abundant relative literature and calibrated as well as corrected based on precipitation as well as temperature similarity. Based on the user manual of the InVEST model, it is assumed that the carbon density of one specific land use is a fixed constant [48].

3) Estimation of Annual Wetland Carbon Storage With WIF: According to the definition of wetlands, wetlands are lands that are permanently, seasonally, or occasionally covered by shallow water, whether natural, or artificial [42], [43], and water is the primary factor controlling the environment in these areas [31], [44]. The presence of water creates conditions that favor the growth of wetland plants and promote the development of

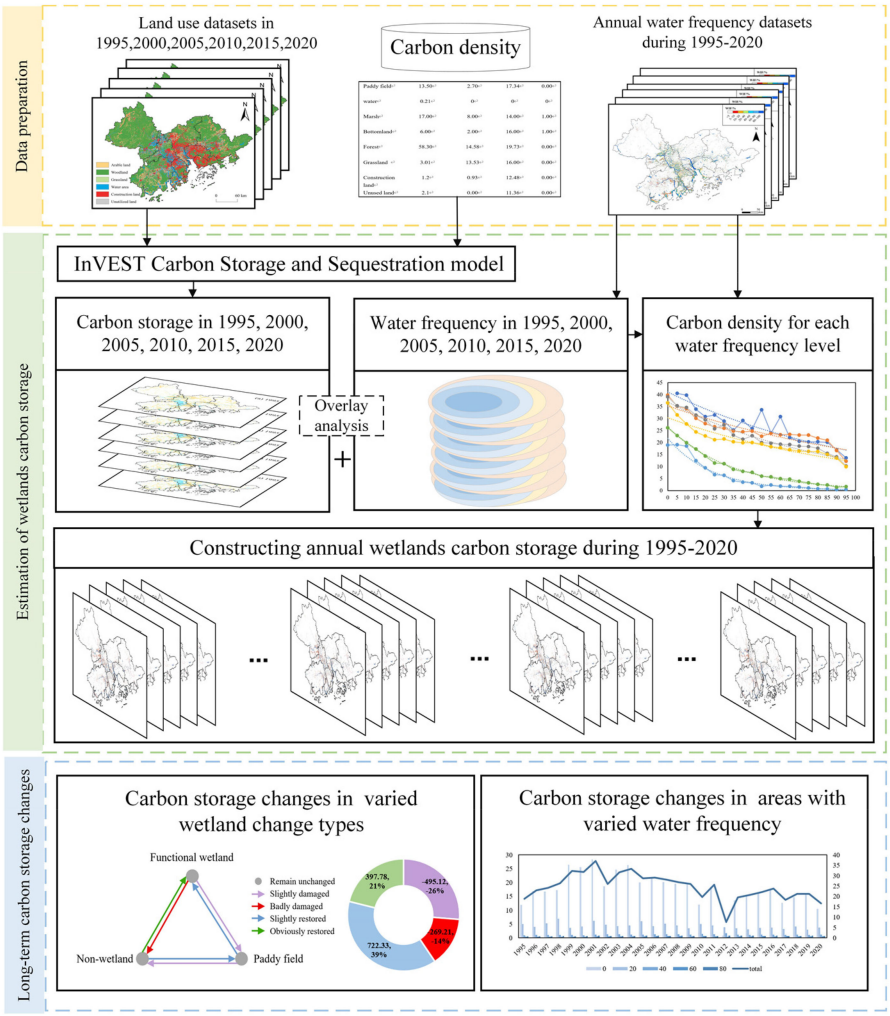

Fig. 2. Flowchart of wetland carbon storage estimation and characterization.

wetland soils, which are closely related with the carbon storage of wetlands [30]. It could be concluded that surface water is an essential component of wetland ecosystems and areas with water occurrence are potential wetland distribution regions.

To refine the estimation of carbon storage in wetlands to a temporal granule of yearly, we developed a method to indirectly evaluate the carbon storage of wetland ecosystems by incorporating WIF information. The WIF index indicates the frequency of water body occurrence in a given pixel during a certain period of time. The WIF could be calculated as follows [38], [45]:

$$\mathrm{WIF} = \frac{\sum_{i=1}^{N} (\varepsilon_i = 1)}{N} \times 100\% \tag{2}$$

where ε_i denotes the pixel value of the ith water map, where 1 is water and 0 is nonwater; $\sum_{i=1}^{N} (\varepsilon_i = 1)$is the total number of observations of water body occurrence during a certain period of time, and N is the total number of valid observations at a specific pixel. We calculated the annual WIF time series in the GBA during 1995–2020, which could represent the potential extent of wetlands for each year in the same period.

To reduce uncertainty and obscurity, the value of WIF is divided into ten levels at 5% intervals. We attempt to investigate the underlying relationship between wetland carbon storage and WIF levels based on an exponential regression model. The schematic representation and photos of transitional wetlands in the potential distribution extent for wetlands alongside the variations in WIF are shown in Fig. 3, which demonstrates that WIF could be used to constrain the extent and predict probable types for wetlands based on flooding frequency to a certain degree. When an area is flooded all year around, it is most likely to be permanent lake or river. When seasonally or occasionally being flooded, there are good chance that an area belongs to tidal flat, marsh, or swamp.

4) Identification of Wetland Change Types: The wetland types of the GBA include rivers, lakes, paddy fields, marshes, reservoirs and ponds, marshes, and floodplain. This study did not include mangrove wetlands due to the fact that the mangrove within the administrative boundary in the GBA is relatively scarce. Differing wetland types have different wetland functions. Among them, rivers and lakes, marsh, and floodplain are natural wetlands that have higher wetland functions and rich

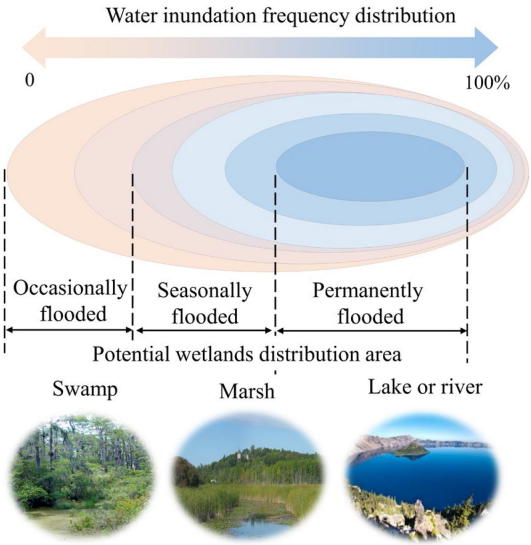

Fig. 3. Schematic representation and photos of transitional wetlands in the potential distribution extent for wetlands.

TABLE II
DEFINITION AND TYPES OF WETLAND DAMAGE DEGREE

T_1-T_2		T_2		
		Functional wetland	Paddy field	Non-wetland
T_1	Functional wetland	Remain unchanged	Slightly damaged	Badly damaged
	Paddy field	Slightly restored	Remain unchanged	Slightly damaged
	Non-wetland	Obviously restored	Slightly restored	Remain unchanged

Note: T_1 and T_2 represent the start and end years, respectively

biodiversity. Reservoirs and ponds and paddy fields belong to artificial wetlands that have lower ecological functions than natural wetlands [49]. However, the ecological functional value of wetlands in paddy fields is higher than that of nonwetlands. The nonwetlands in this study include forest, grassland, construction land, and unused land. Zhang et al. [49] and Long et al. [50] believed that the conversion of wetlands into paddy fields and the conversion of paddy fields into nonwetlands could be considered a kind of damage. To better analyze the damage or recovery degree of wetland changes in the GBA, we set a definition of five types for wetland changes. The definition of these wetland change types is shown in Table II.

III. RESULTS

A. Wetland Carbon Storage Estimation and Spatiotemporal Analysis

The spatial distribution of the carbon storage of wetlands in the GBA during 1995–2020 is illustrated in Fig. 4. The values of wetland carbon storage in Fig. 4 were calculated it by multiplying the area for each 30 m-resolution pixel (900 m^2) and the sum of four types of carbon densities (aboveground, belowground, soil organic, and dead organic matter carbon densities, listed in Table II) for various wetland type. The value for carbon storage in wetlands ranged from 0.17 to 27.17 Mg per pixel, and the distribution of carbon storage in paddy fields decreased considerably after 2000. In addition, the values of carbon storage in different wetland types in 1995, 2000, 2005, 2010, 2015, and 2020 are shown in Fig. 5. Generally, the total carbon storage in wetlands in the GBA fell gradually from 33.38 Tg·C in 1995 to 16.64 Tg·C in 2020, with a significant linear downward trend ($R^2 = 0.9021$) and a decreasing speed of approximately 369.84×10^4 Mg per year. It is also noticeable that the variations in total carbon storage in wetlands of the GBA are maintaining similar values with those in paddy fields, of which the area changed most obviously among all wetland types in the past decades. Moreover, the changing trend of the paddy field area is similar to that of the total carbon storage in wetlands, which indicates that the variations in carbon storage in wetland ecosystems are mainly due to changes in paddy fields over the recent 25-year period. The significant losses of carbon storage in wetlands were mainly owing to intensified anthropologic activities during the study period.

B. Estimation and Analysis of Annual Wetland Carbon Storage With WIF

Given that the annual surface WIF datasets are available between 1995 and 2020, while annual wetland maps are lacking during the same period, we attempted to investigate the potential relationship between the carbon storage in terrestrial ecosystems and WIF intervals to indirectly estimate the annual carbon storage of wetlands in the GBA. As shown in Fig. 6, the carbon storage of terrestrial ecosystems in the six periods of 1995, 2000, 2005, 2010, 2015, and 2020 (derived in results A) under various water inundation frequencies (0%–100%, with 5% intervals) showed relatively similar variations and patterns. After a rapid rise during WIF ranged from 0% to 10%, the carbon storage decreased steeply when the WIF increased gradually at a 5% pace and then remained almost the same in areas with water inundation frequencies ranging roughly between 20% and 80%, but it depicted a slight upward tendency in areas with water inundation frequencies above 85%. This phenomenon is mainly due to the reality that the area of region where WIF>85% is much larger than other regions with WIF ranging from 20% and 85% (as shown in Fig. 6), which is caused by the relatively larger proportion of surface water bodies among all wetland types and the carbon storage under differing WIF in Fig. 6 is the total amount. The areas with various water inundation frequencies showed an obvious "U-shape" characteristic, while the carbon storage presented an overall falling trend with the WIF growing, which is logical.

By overlying the WIF spatial distribution map and corresponding terrestrial ecosystem carbon storage in 1995, 2000, 2005, 2010, 2015, and 2020, the carbon density under varied levels of the water inundation interval could be calculated by the total carbon storage divided by the area with a specific WIF interval. The results of the carbon density of wetlands for different intervals are shown in Fig. 7. It is noteworthy that the change trends of carbon density along with WIF are well fitted with exponential functions, with R^2 values of 0.9576, 0.9604,

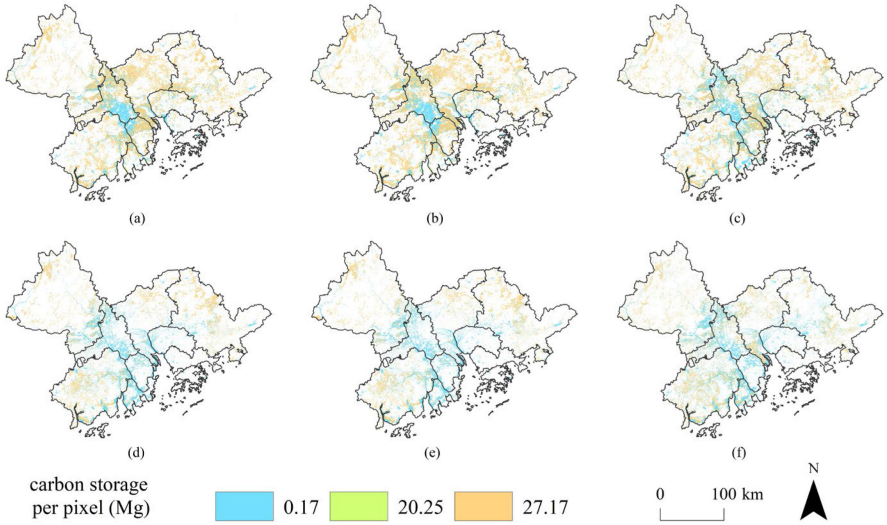

Fig. 4. Spatial distribution of carbon storage for wetlands in the GBA for 1995, 2000, 2005, 2010, 2015, and 2020.

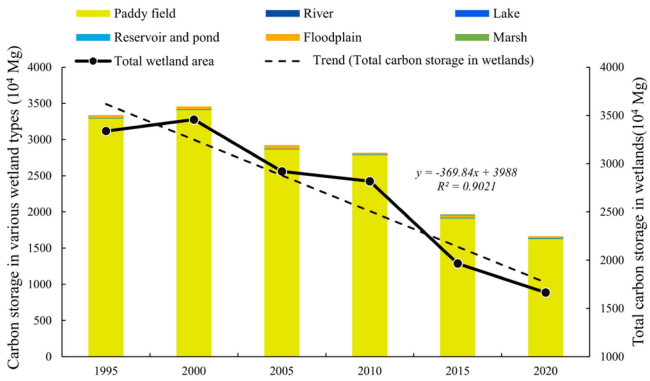

Fig. 5. Carbon storage changes in various wetland types in the GBA during 1995–2020.

and 0.9962 in 2000, 2015, and 2020, respectively. Theoretically, the downward trend of carbon density along with the growth of WIF is consistent with the actual situation, since the carbon storage in water is scarce. However, the inconsistency and uncertainties of land use maps might cause disparities in different years, especially after 2010.

To estimate the annual wetland carbon storage in the GBA during 1995–2020, the exponential function in the neighboring year is applied to the annual WIF time series to retrieve the carbon storage density. Then, we multiplied the carbon density and the area for each pixel (30 m×30 m) to obtain the carbon for each pixel and add it up to derive the total amount of carbon storage for wetlands in each year during 1995–2020. As shown in Fig. 8, there were three kinds of obvious change trends from 1995 to 2020. First, an evident linear upward trend in the carbon storage could be clearly seen during 1995–2004, with an R^2 of 0.754 and a speed of 27.213×10^4 Mg per year. The year 2004 witnessed a rapid decrease until 2013, with an R^2 of 0.7129 and a speed of 25.899×10^4 Mg per year. After 2013, the estimated carbon storage of wetlands displayed a slight fluctuation and remained relatively steady around 250×10^4 Mg. Furthermore, it should be noted that the year 2012's sharp drop in carbon storage, which could be attributed to the sparse amount of Landsat images in this year caused by the stopping of Landsat 5 TM. It could also be easily seen that the change in carbon storage in areas with water frequencies between 0% and 20% accounted for the vast majority of the changes in total carbon storage in wetlands in the GBA.

Furthermore, the yearly continuous spatial pattern storage for wetlands during 1995–2020 is retrieved based on available annual WIF datasets and the corresponding carbon density for each WIF interval calculated. The schematic representation for the time series estimated carbon storage in wetlands and some spatial distributions of wetland carbon storage in 1998, 2003, 2008, 2013, 2018, and 2019 is shown in Fig. 9.

C. Carbon Storage Changes in Various Wetland Change Types

We calculated the carbon storage changes in various wetland types and six change periods to quantify the change characteristics in more detail. Fig. 10 shows wetland carbon storage variation in the periods 1995–2000, 2000–2005, 2005–2010, 2010–2015, 2015–2020, and 1995–2020. Over the period of 1995–2020, the carbon storage of wetlands in slightly damaged region accounted for over half (54%) of the total changed amount, with 7.1×10^4 Mg carbon storage lost, and the vast majority of net decreased wetland carbon storage. During 1995–2000, the net increased carbon storage in wetlands was the highest at 50.81×10^4 Mg, while the net decreased carbon storage in wetlands was the highest at 31.96×10^4 Mg from 2005 to 2010.

The estimated wetland carbon storage in varied water inundation intervals for five types of wetland changes is calculated as well, which is depicted in Fig. 11. As indicated in the figures, the change trend in wetland carbon storage within slightly or obviously restored areas is relatively slow. On the other hand, the change trend in wetland carbon storage in slightly and badly damaged areas presents a more dramatic downward trend during

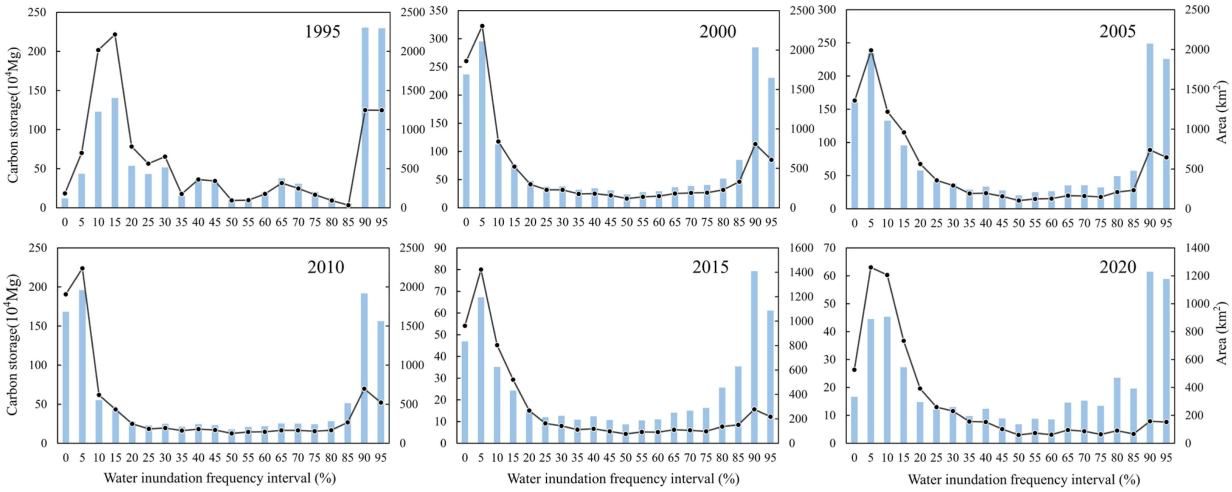

Fig. 6. Carbon storage of wetlands for different WIF intervals from 1995 to 2020.

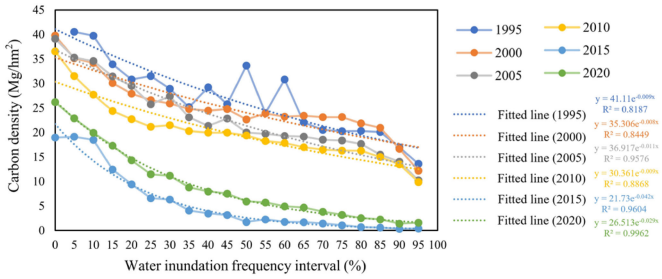

Fig. 7. Carbon storage density of wetlands for different WIF intervals from 1995 to 2020.

2004–2020. It is also noticeable that the magnitude of changes in estimated wetland carbon storage in badly damaged and obviously restored areas is lower (less than 15×10^4 Mg) than that (less than 40×10^4 Mg) in slightly damaged and restored areas, respectively. These results indicate that more attention should be given to slightly damaged areas to prevent wetlands from destruction and degradation.

IV. Discussion

A. Comparison With Other Studies

Comparing this study with previous studies on wetland carbon storage estimation and spatiotemporal analysis [17]–[19], which put more emphasis on terrestrial ecosystem carbon storage estimation, the assessment for wetland carbon storage in this study is more refined and targeted for wetland ecosystems. Furthermore, the evaluation results of wetland carbon storage have a long time series(1995–2020) and higher temporal frequency (yearly) compared with existing studies, which could reflect more detailed and comprehensive spatiotemporal changes of wetland carbon storage in the GBA.

Additionally, the wetland carbon storage framework proposed in this study is innovative and could be easily applied to other similar areas, which is scarce in previous studies. Although the estimation results include some uncertainties, the mechanism behind them is still reasonable and could provide a convenient and efficient means for acquiring long-term wetland carbon storage time series through WIF datasets generated on the GEE platform and corresponding exponential function relationships.

B. Implications for Wetland Carbon Management in the GBA

The timeline of some important wetland-related policies and economic plans in China is illustrated in Fig. 12. With increased awareness and valuation of wetland carbon sequestration, the protection and recovery of wetlands in China have received much more attention in recent years. According to the China wetland conservation action plan (released in 2000), China, aims to curb the shrinking trend of natural wetlands caused by human activities by 2010 and gradually restore degraded or lost wetlands by 2020. The national wetland protection plan (2004–2030) approved by the State Council in 2003 proposes that more than 90% of natural wetlands will be effectively protected by 2030. These wetland-related policies have exerted beneficial effects on wetlands protection and recovery. However, the impact of urbanization and socioeconomic-related human activities on wetlands in recent decades are also nonnegligible.

By comparing the timeline of wetland-related policies and economic urbanization plans with wetland carbon storage changes during 1995–2020, some interesting coincidences could be found. After the launch of the Plan for Ecological Environmental Conservation in China in 1998, wetland carbon storage increased more dramatically than it did in the previous year (seen in Fig. 8). The year 2001, in which China joined the WTO, witnessed a drop in wetland carbon storage from in the GBA. Until 2012, when ecological civilization construction was adopted as a national policy, the carbon storage of wetlands began to rise and fluctuate between 200 and 300 $\times 10^4$ Mg during subsequent years. The relatively balanced status might be caused by the counteraction of the new urbanization strategy implemented and the ecological red line of wetland conservation identified for wetland conservation. Furthermore, the results of this study could be used as references in wetland-related action

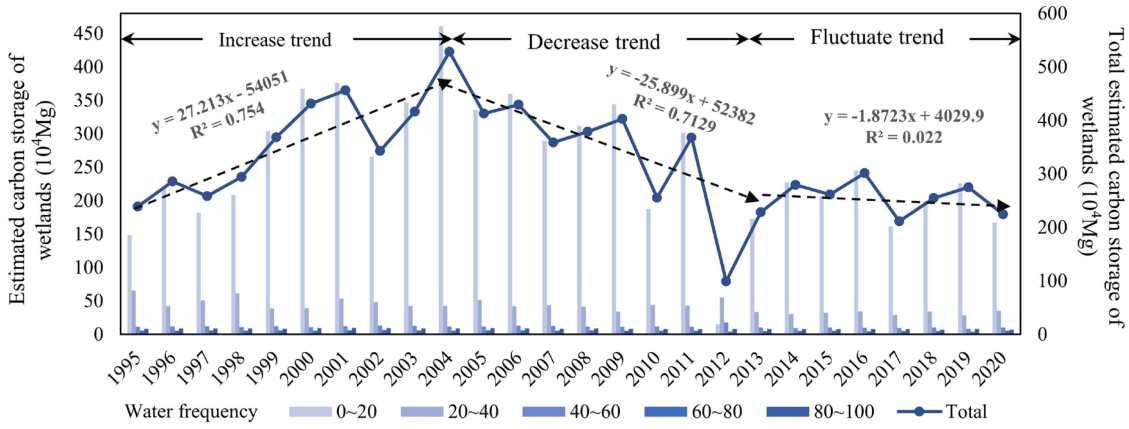

Fig. 8. Carbon storage changes in wetlands for different WIF intervals from 1995 to 2020.

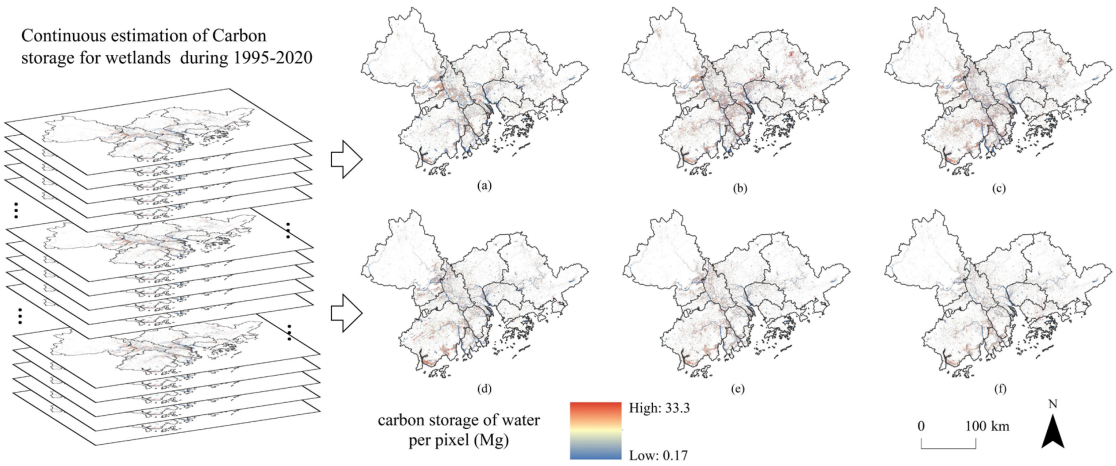

Fig. 9. Illustration of annual estimated carbon storage in wetlands and some spatial patterns of estimated wetland carbon storage in 1998, 2003, 2008, 2013, 2018, and 2019.

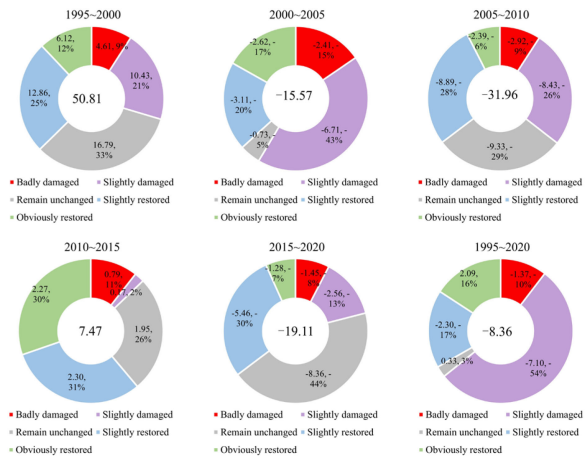

Fig. 10. Changes in wetland carbon storage (unit: 10^4 Mg) in various change types.

plans' decision-making, which could help identify areas, which need urgent protection and recovery efficiently.

C. Limitations and Potential Improvements of This Study

There are also some limitations and uncertainties in this study. Some intrinsic uncertainties in calculating carbon storage exists in the InVEST model. First, the model calculates the carbon storage and its temporal and spatial variation based on land use type changes but does not consider many other factors, such as photosynthetic rate and soil microbial activities, which have important effects on carbon sequestration. Second, there is no interannual change in carbon density in this model, which leads to the fact that the change in carbon storage is caused by the transformation of land use type. Finally, the land use types are classified based on remote sensing images. Although remote sensing technology is becoming increasingly advanced, there are still some systematic or random errors in the accuracy of land use classification because of the effects of cloud, cloud shadow and subjective errors induced by visual interpretation and other processes.

Additionally, the corresponding relations between WIF and carbon storage of wetlands might not be suitable when applied in other study areas due to the discrepancy among regions

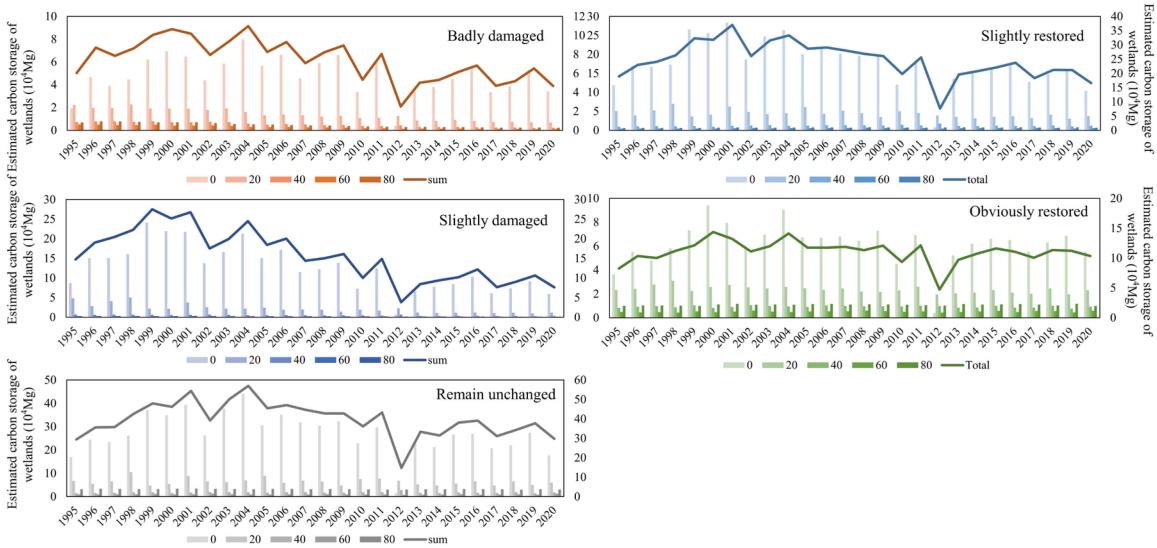

Fig. 11. Changes in wetland carbon storage in varied change types under different WIF intervals.

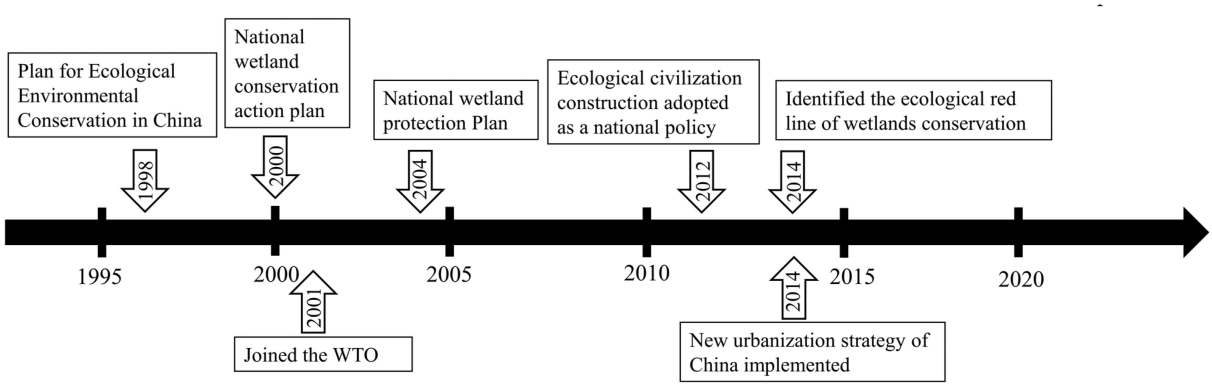

Fig. 12. Timeline of wetland-related policies and China's economic plans.

with varied climate and vegetation conditions. Although some uncertainty exists in the InVEST model, the results could clearly reflect the spatiotemporal variations in carbon storage in the GBA in recent decades, which could be an indicator of regional ecosystem service function to some extent.

In future research, we will reinforce carbon density monitoring for different wetland classes and boost the accuracy and spatial resolution of land use classification. Considering that the carbon storage calculation module only takes carbon density for varied classes and excludes the spatial heterogeneity in different classes, the assessment changes with the land use changes. Thus, future research should strengthen the continuous monitoring of carbon density in the field.

V. Conclusion

In this study, in order to improve the understanding of carbon storage changes in wetland ecosystems in the GBA, we estimated annual wetland carbon storage from 1995 to 2020 based on InVEST model and yearly WIF calculated from Landsat time series on the GEE platform. Additionally, the spatiotemporal dynamics of carbon storage in wetlands of the GBA was characterized by five wetland change types. The main conclusion drawn in this study are as follows.

1) The carbon storage of wetlands estimated by the InVEST model based on land use maps showed a slow decreasing trend from 33.38 to 16.64 Tg·C during 1995–2020. The regions with larger carbon storage are generally distributed in regions around river networks or flooded areas, with a higher potential of being classified as marsh or swamp.
2) The relationship between WIF and carbon storage density within the potential region of wetland distribution for 2005, 2015, and 2020 is surprisingly fitted in exponentially decreasing functions with R^2 values of 0.9576, 0.9604, and 0.9962, respectively. This variation is in accordance with the transition characteristics of wetland types when the probability of being water is rising.
3) The temporal changes in wetland carbon storage could be divided into three main stages, a rapidly increasing period, a steeply falling period, and a slightly fluctuating period, during which when wetland-related conservation and economic policies played a vital role. The time points

of policies implemented are relatively consistent with the turning points of wetland carbon storage variations.

4) The wetland carbon storage in badly damaged areas shows a more obvious decreasing trend than in other types. Furthermore, the main changes occurred in regions with water inundation frequencies less than 20%.

Additionally, the estimated long-term wetland carbon storage datasets and spatiotemporal analysis results could be provided as scientific references for local government' s or institutions' decision-making, which relates to wetland protection, restoration and management as well as carbon neutrality strategies. Furthermore, the proposed methodology and framework for assessing the carbon storage of wetlands could be easily applied in other regions worldwide to support the monitoring and conservation of wetlands' ecological status and functions and understanding the spatiotemporal evolution characteristics of regional carbon stocks.

ACKNOWLEDGMENT

The author would like to thank the editors and anonymous reviewers for their useful and valuable suggestions.

REFERENCES

[1] D. Xiao, L. Deng, D. G. Kim, C. Huang, and K. Tian, "Carbon budgets of wetland ecosystems in China," *Glob. Change Biol.*, vol. 25, no. 6, pp. 2061–2076, 2019.

[2] A. M. Nahlik and M. S. Fennessy, "Carbon storage in US wetlands," *Nature Commun.*, vol. 7, no. 1, 2016, Art. no. 13835.

[3] X. Ouyang and S. Y. Lee, "Improved estimates on global carbon stock and carbon pools in tidal wetlands," *Nature Commun.*, vol. 11, no. 1, 2020, Art. no. 317.

[4] T. Mazurczyk and R. P. Brooks, "Carbon storage dynamics of temperate freshwater wetlands in Pennsylvania," *Wetlands Ecol. Manage.*, vol. 26, no. 5, pp. 893–914, Jan. 2018.

[5] Y. Li, J. Qiu, Z. Li, and Y. Li, "Assessment of blue carbon storage loss in coastal wetlands under rapid reclamation," *Sustainability*, vol. 10, no. 8, Aug. 2018, Art. no. 2818.

[6] S. van Asselen, P. H. Verburg, J. E. Vermaat, and J. H. Janse, "Drivers of wetland conversion: A global meta-analysis," *PLoS One*, vol. 8, no. 11, Jan. 2013, Art. no. e81292.

[7] D. Mao et al., "China's wetlands loss to urban expansion," *Land Degradation Develop.*, vol. 29, no. 8, pp. 2644–2657, Jan. 2018.

[8] D. Mao et al., "National wetland mapping in China: A new product resulting from object-based and hierarchical classification of landsat 8 OLI images," *ISPRS J. Photogrammetry*, vol. 164, pp. 11–25, Jan. 2020.

[9] M. A. Young, O. Serrano, P. I. Macreadie, C. E. Lovelock, P. Carnell, and D. Ierodiaconou, "National scale predictions of contemporary and future blue carbon storage," *Sci. Total Environ.*, vol. 800, 2021, Art. no. 149573.

[10] G. Zhu et al., "Land-use changes lead to a decrease in carbon storage in arid region, China," *Ecological Indicators*, vol. 127, Jan. 2021, Art. no. 107770.

[11] H. X. Liu, H. Ren, D. F. Hui, W. Q. Wang, B. W. Liao, and Q. X. Cao, "Carbon stocks and potential carbon storage in the mangrove forests of China," *J. Environ. Manage.*, vol. 133, pp. 86–93, Jan. 2014.

[12] C. E. Lovelock et al., "Contemporary rates of carbon sequestration through vertical accretion of sediments in mangrove forests and saltmarshes of South East Queensland, Australia," *Estuaries Coasts*, vol. 37, no. 3, pp. 763–771, Jan. 2014.

[13] X. Sun and F. Li, "Spatiotemporal assessment and trade-offs of multiple ecosystem services based on land use changes in Zengcheng, China," *Sci. Total Environ.*, vol. 609, pp. 1569–1581, Jan. 2017.

[14] X. Liu et al., "Impacts of urban expansion on terrestrial carbon storage in China," *Environ. Sci. Technol.*, vol. 53, no. 12, pp. 6834–6844, Jun. 2019.

[15] W. Jiang, Y. Deng, Z. Tang, X. Lei, and Z. Chen, "Modelling the potential impacts of urban ecosystem changes on carbon storage under different scenarios by linking the CLUE-S and the InVEST models," *Ecol. Model.*, vol. 345, pp. 30–40, 2017.

[16] Y. J. Liang, L. J. Liu, and J. J. Huang, "Integrating the SD-CLUE-S and InVEST models into assessment of oasis carbon storage in Northwestern China," *PLoS One*, vol. 12, no. 2, Jan. 2017, Art. no. e0172494.

[17] C. Y. He, D. Zhang, Q. X. Huang, and Y. Y. Zhao, "Assessing the potential impacts of urban expansion on regional carbon storage by linking the LUSD-urban and InVEST models," *Environ. Model. Softw.*, vol. 75, pp. 44–58, Jan. 2016.

[18] D. Babbar, G. Areendran, M. Sahana, K. Sarma, K. Raj, and A. Sivadas, "Assessment and prediction of carbon sequestration using Markov chain and InVEST model in Sariska Tiger Reserve, India," *J. Cleaner Prod.*, vol. 278, Jan. 2021, Art. no. 123333.

[19] L. Guo et al., "Mapping soil organic carbon stock by hyperspectral and time-series multispectral remote sensing images in low-relief agricultural areas," *Geoderma*, vol. 398, 2021, Art. no. 115118.

[20] H. Liu, P. Gong, J. Wang, N. Clinton, Y. Bai, and S. Liang, "Annual dynamics of global land cover and its long-term changes from 1982 to 2015," *Earth Syst. Sci. Data*, vol. 12, no. 2, pp. 1217–1243, Jun. 2020.

[21] X. Zhang, L. Liu, X. Chen, Y. Gao, S. Xie, and J. Mi, "GLC_FCS30: Global land-cover product with fine classification system at 30 m using time-series landsat imagery," *Earth System Sci. Data*, vol. 13, no. 6, pp. 2753–2776, Jun. 2021.

[22] N. Gorelick, M. Hancher, M. Dixon, S. Ilyushchenko, D. Thau, and R. Moore, "Google Earth Engine: Planetary-scale geospatial analysis for everyone," *Remote Sens. Environ.*, vol. 202, pp. 18–27, 2017.

[23] M. Amani et al., "Google Earth Engine cloud computing platform for remote sensing big data applications: A comprehensive review," *IEEE J. Sel. Topics Appl. Earth Observ. Remote Sens.*, vol. 13, pp. 5326–5350, 2020, doi: 10.1109/JSTARS.2020.3021052.

[24] X. Wang et al., "Mapping coastal wetlands of China using time series landsat images in 2018 and Google Earth Engine," *ISPRS J. Photogrammetry*, vol. 163, pp. 312–326, 2020.

[25] Y. Zhou et al., "Continuous monitoring of lake dynamics on the Mongolian Plateau using all available landsat imagery and Google Earth Engine," *Sci. Total Environ.*, vol. 689, pp. 366–380, 2019.

[26] Y. Deng, W. Jiang, Z. Tang, Z. Ling, and Z. Wu, "Long-Term changes of open-surface water bodies in the yangtze river basin based on the Google Earth Engine cloud platform," *Remote Sens.*, vol. 11, no. 19, Sep. 2019, Art. no. 2213.

[27] Y. Deng et al., "Spatio-Temporal change of lake water extent in Wuhan urban agglomeration based on landsat images from 1987 to 2015," *Remote Sens.*, vol. 9, no. 3, Mar. 2017, Art. no. 270.

[28] C. Wang, W. Jiang, Y. Deng, Z. Ling, and Y. Deng, "Long time series water extent analysis for SDG 6.6.1 based on the GEE platform: A case study of dongting lake," *IEEE J. Sel. Topics Appl. Earth Observ. Remote Sens.*, vol. 15, pp. 490–503, 2022, doi: 10.1109/JSTARS.2021.3088127.

[29] F. Deng et al., "Analysis of the relationship between inundation frequency and wetland vegetation in dongting lake using remote sensing data," *Ecohydrology*, vol. 7, no. 2, pp. 717–726, 2014.

[30] J. Z. Coletti, C. Hinz, R. Vogwill, and M. R. Hipsey, "Hydrological controls on carbon metabolism in wetlands," *Ecol. Model.*, vol. 249, pp. 3–18, Jan. 2013.

[31] L. M. Cowardin, V. Carter, F. C. Golet, and E. T. Laroe, "Classification of wetlands and deepwater habitats of the United States," FWS/OBS, Washington, DC, USA, Tech. Rep. FWS/OBS-79/31, 1979.

[32] C. Yang et al., "Rapid urbanization and policy variation greatly drive ecological quality evolution in Guangdong-Hong Kong-Macau Greater Bay Area of China: A remote sensing perspective," *Ecological Indicators*, vol. 115, 2020, Art. no. 106373.

[33] Y. Wang, Y. Yao, S. Chen, Z. Ni, and B. Xia, "Spatiotemporal evolution of urban development and surface urban heat island in Guangdong-Hong Kong-Macau Greater Bay Area of China from 2013 to 2019," *Resour., Conservation Recycling*, vol. 179, 2022, Art. no. 106063.

[34] L. Shi, H. Taubenböck, Z. Zhang, F. Liu, and M. Wurm, "Urbanization in China from the end of 1980s until 2010—spatial dynamics and patterns of growth using EO-data," *Int. J. Digit. Earth*, vol. 12, no. 1, pp. 78–94, 2019.

[35] Y. Lu, J. Yang, M. Peng, T. Li, D. Wen, and X. Huang, "Monitoring ecosystem services in the Guangdong-Hong Kong-Macao Greater Bay Area based on multi-temporal deep learning," *Sci. Total Environ.*, vol. 822, 2022, Art. no. 153662.

[36] Y. Li, W. Wang, M. Chang, and X. Wang, "Impacts of urbanization on extreme precipitation in the Guangdong-Hong Kong-Macau Greater Bay Area," *Urban Climate*, vol. 38, 2021, Art. no. 100904.

[37] H. Weng, J. Kou, and Q. Shao, "Evaluation of urban comprehensive carrying capacity in the Guangdong–Hong Kong–Macao Greater Bay Area based on regional collaboration," *Environ. Sci. Pollut. Res.*, vol. 27, no. 16, pp. 20025–20036, Jan. 2020.
[38] Y. Deng, W. Jiang, Z. Wu, Z. Ling, K. Peng, and Y. Deng, "Assessing surface water losses and gains under rapid urbanization for SDG 6.6.1 using long-term landsat imagery in the Guangdong-Hong Kong-Macao Greater Bay Area, China," *Remote Sens.*, vol. 14, no. 4, 2022, Art. no. 881.
[39] S. K. McFeeters, "The use of the normalized difference water index (NDWI) in the delineation of open water features," *Int. J. Remote Sens.*, vol. 17, no. 7, pp. 1425–1432, 1996.
[40] H. Xu, "Modification of normalised difference water index (NDWI) to enhance open water features in remotely sensed imagery," *Int. J. Remote Sens.*, vol. 27, no. 14, pp. 3025–3033, 2006.
[41] G. L. Feyisa et al., "Automated water extraction index: A new technique for surface water mapping using landsat imagery," *Remote Sens. Environ.*, vol. 140, pp. 23–35, 2014.
[42] O. M. Bragg, "Hydrology of peat-forming wetlands in Scotland," *Sci. Total Environ.*, vol. 294, no. 1, pp. 111–129, Jan. 2002.
[43] M. Guo, J. Li, C. Sheng, J. Xu, and L. Wu, "A review of wetland *remote sensing*," *Sensors*, vol. 17, no. 4, 2017, Art. no. 777.
[44] L. Yang et al., "Four decades of wetland changes in dongting lake using landsat observations during 1978–2018," *J. Hydrol.*, vol. 587, 2020, Art. no. 124954.
[45] X. Wang, W. Wang, W. Jiang, K. Jia, P. Rao, and J. Lv, "Analysis of the dynamic changes of the baiyangdian lake surface based on a complex water extraction method," *Water*, vol. 10, no. 11, Nov. 2018, Art. no. 1616.
[46] Z. Zhu, X. Ma, and H. Hu, "Spatio-temporal evolution and prediction of ecosystem carbon stocks in Guangzhou City by coupling FLUS-InVEST models," *Bull. Soil Water Conservation*, vol. 41, no. 2, pp. 222–229. 2021.
[47] T. Ma, X. Li, J. Bai, S. Ding, F. Zhou, and B. Cui, "Four decades' dynamics of coastal blue carbon storage driven by land use/land cover transformation under natural and anthropogenic processes in the yellow river delta, China," *Sci. Total Environ.*, vol. 655, pp. 741–750, 2019.
[48] R. Sharp et al., InVEST Version 3.2. 0 User's Guide. The natural Capital Project. The Nature Conservancy, and World Wildlife Fund. Stanford University, Stanford, CA, USA, University of Minnesota, Minneapolis, MN, USA, 2015.
[49] Z. Zhang, B. Hu, W. Jiang, and H. Qiu, "Identification and scenario prediction of degree of wetland damage in guangxi based on the CA-Markov model," *Ecological Indicators*, vol. 127, 2021, Art. no. 107764.
[50] X. Long, H. Lin, X. An, S. Chen, S. Qi, and M. Zhang, "Evaluation and analysis of ecosystem service value based on land use/cover change in dongting lake wetland," *Ecological Indicators*, vol. 136, 2022, Art. no. 108619.

Yawen Deng received the B.S. degree in geographic information science in 2020 from Beijing Normal University, Beijing, China, where she is currently working toward the master's degree in cartography and geographical information engineering.

Her research interests include surface water mapping and remote sensing of wetlands.

Weiguo Jiang received the B.S. degree in geography from Hunan Normal University, Changsha, China, in 1999, the M.S. degree in physical geography from Nanjing Normal University, Nanjing, China, in 2003, and the Ph.D. degree in cartography and geographical information system from Beijing Normal University, Beijing, China, in 2006.

He is currently a Professor with Beijing Normal University. His research interests include remote sensing, hydrology, and International urban wetland protection and exploration of SDGs.

Zhifeng Wu (Member, IEEE) received the B.S. degree in geography education from Hunan Normal University, Changsha, China, in 1992, the M.S. degree in physical geography from South China Normal University, Guangzhou, China, in 1995, and the Ph.D. degree in cartography and geographical information system from Chinese Academy of Sciences, Beijing, China, in 2002.

He is currently a Professor with Guangzhou University, Guangzhou, China. His research interests include urban remote sensing, terrestrial ecological remote sensing and GIS, and spatiotemporal big data analysis.

Kaifeng Peng received the B.S. degree in remote sensing science and technology from Henan Polytechnic University, Jiaozuo, China, in 2015, and the M.S. degree in surveying and mapping engineering from Wuhan University, Wuhan, China, in 2017. He is currently working toward the Ph.D. degree in remote sensing and GIS with Beijing Normal University.

His research interests include wetland classification, land use simulation, and ecological evaluation.

Ziyan Ling received the B.S. degree in geographic information system in 2008 from Nanjing Forestry University, Nanjing, China, and the M.S. degree in cartography and geographical information system in 2011 from Beijing Normal University, Beijing, China, where she is currently working toward the Ph.D. degree in cartography and GIS.

She is currently a 3S Teaching and Scientific Research with Nanning Normal University, Nanning, China.

Zhuo Li received the B.S. degree in remote sensing science and technology from Capital Normal University, Beijing, China, in 2017. She is currently working toward the Ph.D. degree in cartography and geographical information system with Beijing Normal University, Beijing.

Her research mainly focuses on wetland urban simulation and sustainable development evaluation.

Xiaoya Wang received the B.S. degree in geographic information science from Southeast University, Nanjing, China, in 2017. She is currently working toward the Ph.D. degree in cartography and geographical information system with Beijing Normal University, Beijing, China.

Her research focuses on wetland extraction based on remote sensing.